

The First Stage of Firn Densification - An Evaluation of Grain Boundary Sliding

Timm Schultz^{1,*}, Ralf Müller¹, Dietmar Gross², and Angelika Humbert^{3,4}

¹ Technische Universität Kaiserslautern, Kaiserslautern, Germany

² Technische Universität Darmstadt, Darmstadt, Germany

³ Alfred-Wegener-Institut, Helmholtz-Zentrum für Polar- und Meeresforschung, Bremerhaven, Germany

⁴ Universität Bremen, Bremen, Germany

Firn describes the interstage product between snow and ice in cold regions of the earth, where annual snow fall exceeds the amount of snow melting. The continuing accumulation of snow leads to its densification due to overburden stress until it becomes ice. In the field of glaciology various attempts on simulating firn densification have been made and new models are still developed, as the knowledge of the firn column's density structure allows important derivations.

The presented study reassesses a model description for low density firn based on the process of grain boundary sliding presented by Alley in 1987 [1] using an optimisation approach. By comparing simulation results to 159 measured firn density profiles from Greenland and Antarctica it finds a possible additional dependency of the constitutive relation on the mean surface mass balance. This result is interpreted as an insufficient description of the stress regime.

© 2021 The Authors. *Proceedings in Applied Mathematics & Mechanics* published by Wiley-VCH GmbH.

1 Introduction

Firn densification is mainly driven by stress and temperature and resembles sintering at high temperatures. The presented study focusses on the very first stage of the process, from the snow deposition to a density of $\rho_c = 550 \text{ kg m}^{-3}$ which corresponds to the theoretical value of a dense sphere packing. One of the models for the description of firn densification at low densities is based on grain boundary sliding, introduced by Alley in 1987 [1]. Despite being used in various firn densification models [2–5], the correctness of this model is disputed as observations of inter crystalline deformation in firn are rare [6]. The study aims to test the potential of this model to reproduce measured firn density profiles.

2 Grain Boundary Sliding

For this study a global form of the constitutive relation for grain boundary sliding in firn by Alley (1987) [1] is used. It incorporates a description for the boundary viscosity by Raj & Ashby (1971) [7] and a constant relation of grain radius and neck radius introduced by Arthern & Wingham (1998) [2]:

$$\dot{\epsilon}_{zz} = -\frac{2}{15} \delta_b \frac{8 D_{BD} \Omega}{k_b T h^2} \frac{1}{r \mu^2} \left(\frac{\rho_{ice}}{\rho} \right)^3 \left(1 - \frac{5}{3} \frac{\rho}{\rho_{ice}} \right) t_{zz}, \quad D_{BD} = A_{BD} \exp \left(-\frac{Q_{BD}}{RT} \right). \quad (1)$$

The factor $2/15$ is the result of several geometrical assumptions. δ_b describes the width of the grain boundary. The following factor is the reciprocal boundary viscosity [7] with D_{DB} describing the amount of boundary diffusion in the form of an Arrhenius law, Ω being the volume of the H_2O molecule, Boltzman's constant k_b , the temperature T and the amplitude of grain boundary obstructions h . Latter can be understood as a measure for the roughness of the grain boundaries. The Arrhenius law incorporates the activation energy for boundary diffusion in ice Q_{BD} and a corresponding pre factor A_{BD} as well as the universal gas constant R . The grain radius in firn is denoted by r , whereas μ stands for the ratio of grain radius to neck radius [2]. Furthermore the strain rate in vertical direction $\dot{\epsilon}_{zz}$ depends on the firn density ρ and the stress in vertical direction t_{zz} . The constant $\rho_{ice} = 917 \text{ kg m}^{-3}$ describes the theoretical density of pure ice.

3 Optimisation

The optimisation approach aims to find the best model description for 159 measured firn density profiles from Greenland and Antarctica. All profiles are part of the "SUMup snow density subdataset" [8]. Needed forcing data for temperature and surface mass balance at the locations of the firn profiles are provided by the regional climate model RACMO2.3 [9, 10]. As the surface density can not be derived from all analysed firn profiles, the optimal surface density is identified during the optimisation process.

* Corresponding author: e-mail ttschultz@rhrk.uni-kl.de



This is an open access article under the terms of the Creative Commons Attribution License, which permits use, distribution and reproduction in any medium, provided the original work is properly cited.

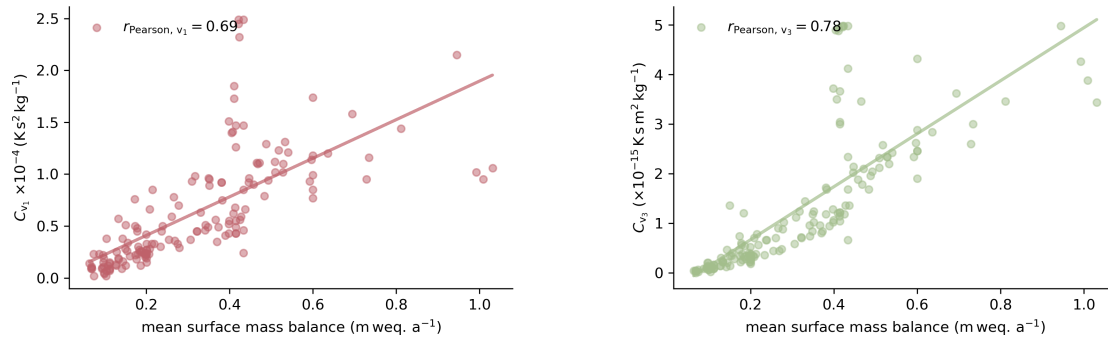


Fig. 1: Factors C_{v_1} (left) and C_{v_3} (right) resulting in the best simulation results for 159 measured firn density profiles from Greenland and Antarctica plotted of the mean surface mass balance at the locations of the measurements. The plots feature the Pearson correlation coefficient r_{Pearson} and a linear fit. Data for the surface mass balance are provided by the regional climate model RACMO2.3 [9, 10].

To find an optimal model description four variants of the constitutive relation (Equation (1)) are formulated. These variants maintain the general structure of the constitutive relation, but sum all material parameters, which might be flawed or show hidden dependencies, in a single factor C . For this publication only two of these variants, variant 1 and variant 3, are discussed:

$$\dot{\epsilon}_{zzv_1} = -C_{v_1} D_{BD} \frac{1}{T} \frac{1}{r} \left(\frac{\rho_{\text{ice}}}{\rho} \right)^3 \left(1 - \frac{5}{3} \frac{\rho}{\rho_{\text{ice}}} \right) t_{zz}, \quad \dot{\epsilon}_{zzv_3} = -C_{v_3} \frac{1}{T} \frac{1}{r} \left(\frac{\rho_{\text{ice}}}{\rho} \right)^3 \left(1 - \frac{5}{3} \frac{\rho}{\rho_{\text{ice}}} \right) t_{zz}. \quad (2)$$

Variant 1 features the Arrhenius law D_{BD} describing the amount of boundary diffusion between ice grains in the firn. This maintains the additional dependency on the temperature T but requires given values for the activation energy Q_{BD} and the pre factor A_{BD} . In contrast to this variant 3 incorporates the Arrhenius law implicitly in the factor C_{v_3} .

For every of the 159 firn profiles the simulation, modelling the density, temperature, grain radius and age of the firn, is run with a range of constant values for the factors C_{v_1} and C_{v_3} . The simulation results are then compared to the measured firn density by calculating the root mean square deviation. In this way individual optimal factors C_{v_1} and C_{v_3} for every location are identified.

4 Results & Discussion

Fig. 1 shows the factors C_{v_1} and C_{v_3} resulting in the best simulation results in relation to the mean surface mass balance computed over the simulation time. The mean surface mass balance shows the strongest linear correlation with the optimal factors identified by the optimisation. We interpret this possible dependency of the optimisation results on the surface mass balance as an insufficient description of the stress regime. The common one dimensional simulation approach in firn density modelling neglects horizontal components of the stress tensor acting on the firn. A modelling approach considering these additional stress components however requires an adjustment of the constitutive relation. A modified constitutive relation has to incorporate the shear viscosity as well as the bulk viscosity [11]. This will be the subject of future work.

Acknowledgements This work has been funded by the German Research Foundation (project number: 403642112), it is part of the priority program 1158 “Antarctic Research with Comparative Investigations in Arctic Ice Areas”. Open access funding enabled and organized by Projekt DEAL.

References

- [1] R. B. Alley, *Journal de Physique* **48**(C1), C1–249 – C1–256 (1987).
- [2] R. J. Arthern and D. J. Wingham, *Climatic Change* **40**, 605–624 (1998).
- [3] L. Arnaud, J. M. Barnola, and P. Duval, *Physics of Ice Core Records* pp. 285–305 (2000).
- [4] C. Goujon, J. M. Barnola, and C. Ritz, *Journal of Geophysical Research* **108**(D24), 4792 (2003).
- [5] C. Bréant, P. Marinerie, A. Orsi, L. Arnaud, and A. Landais, *Clim. Past*, **13**, 833–853 (2017).
- [6] T. Theile, H. Löwe, T. C. Theile, and M. Schneebeli, *Acta Materialia* **59**, 7104–7113 (2011).
- [7] R. Raj and M. F. Ashby, *Metallurgical Transactions* **2**, 1113–1127 (1971).
- [8] L. Koenig and L. Montgomery, *Surface mass balance and snow depth on sea ice working group (sumup) snow density subdataset, greenland and antarctica, 1950–2018*, Tech. rep., Arctic Data Center, 2019.
- [9] J. M. Van Wessel, C. H. Reijmer, M. Morlighem, J. Mougnot, E. Rignot, B. Medley, I. Joughin, B. Wouter, M. A. Depoorter, J. L. Bamber, J. T. M. Lenaerts, W. J. Van De Berg, M. R. Van Den Broeke, and E. Van Meijgaard, *Journal of Glaciology* **60**(222), 761–770 (2014).
- [10] B. Noël, W. J. van de Berg, E. van Meijgaard, P. Kuipers Munneke, R. S. W. van de Wal, and M. R. van den Broeke, *The Cryosphere* **9**(5), 1831–1844 (2015).
- [11] R. Greve and H. Blatter, *Dynamics of Ice Sheets and Glaciers*, *Advances in Geophysical and Environmental Mechanics and Mathematics* (Springer-Verlag, Berlin Heidelberg, 2009).